

Conjugated Polymers Containing Mixed-Ligand Ruthenium(II) Complexes. Synthesis, Characterization, and Investigation of Photoconductive Properties

Qing Wang and Luping Yu*

Contribution from the Department of Chemistry and James Franck Institute, The University of Chicago, 5735 South Ellis Avenue, Chicago, Illinois 60637

Received August 22, 2000

Abstract: A series of novel conjugated polymers containing mixed-ligand ruthenium complexes has been synthesized and characterized. These polymers exhibit interesting photoconductive properties. It was found that the redox and optical properties of the resulting materials were strongly affected by the structures of coordinated ligands of the ruthenium complex. The presence of σ -donating diketonate and phenolate groups in ligands substantially lowered the Ru(III/II) potentials relative to analogous polypyridyl complexes. A range of transition energies of metal-to-ligand charge transfer was observed. The photoconductivity of the polymer at long wavelengths is strongly enhanced by the metal complexes due to the metal-to-ligand charge-transfer transition.

Introduction

Hybrid polymers containing both organic and inorganic components have recently been pursued by many groups for a variety of applications.^{1–3,5} One of the most attractive systems is the conjugated polymers containing transition metal complexes. Introduction of transition metal ions into π -conjugated polymers provides enormous opportunities to tune the physical properties of the resulting materials. From the strong interaction between transition metal complexes and conducting polymer backbones, unique photophysical, photochemical, and electrochemical properties are expected to evolve, leading to materials with a wide range of interesting physical properties, such as photorefractive effects, photoconductivity, and novel redox property.^{1–3} Ruthenium(II) polypyridine complexes are among the most studied molecules due to their rich and well-

characterized photophysics and redox chemistry.⁴ The polymers derived from these complexes have been demonstrated promising potential for applications in solar energy conversion, sensor, polymer supported electrode, nonlinear optics, photorefractive, and electroluminescence.^{1,5}

Our research group has been interested in these hybrid materials for a long time.¹ We want to utilize the rich photochemical and photophysical phenomena in these metal-containing conjugated polymers for photorefractive applications and for harvesting light energy.⁶ Therefore, poly(*p*-phenylenevinylene) (PPV) functionalized with various transition metal complexes such as tris(bipyridyl)ruthenium and tris(bipyridyl)osmium,¹ metalloporphyrin, and metallophthalocyanine were synthesized.⁷ The resulting polymers have shown enhanced photoconductivity and higher quantum yield of photocharge generation than those without metal complexes.

An attractive feature that these systems offer is the flexibility in fine-tuning the optical and electronic properties of resultant materials. Simple change in the transition metal centers or the ligands can lead to a significant modulation of the physical properties of the resulting polymers. However, to achieve this flexibility, syntheses of proper monomers and suitable polymerization methods are required. For example, ruthenium complexes of polypyridine such as 2,2'-bipyridine (bpy) and 2,2':6',2''-terpyridine (tpy) have been the favored complexes for polymerization because they are compatible with Pd-catalyzed coupling and electrochemical coupling.¹ There are far fewer investigations of the effect of ligand modification. To extend the chemistry of the well-known polypyridine ligands, this paper reports the synthesis of a series of novel ruthenium complexes containing β -diketonate and hydroxyquinoline ligands and the integration of them into PPV main chains. It was found that

(1) (a) Peng, Z.; Yu, L. *J. Am. Chem. Soc.* **1996**, *118*, 3777. (b) Peng, Z.; Gharavi, A.; Yu, L. *J. Am. Chem. Soc.* **1997**, *119*, 4622. (c) Wang, Q.; Wang, L.; Yu, L. *J. Am. Chem. Soc.* **1998**, *120*, 12860.

(2) (a) Hirao, T.; Higuchi, M.; Yamaguchi, S. *Macromol. Symp.* **1998**, *131*, 59. (b) Pickup, P. G. *J. Mater. Chem.* **1999**, *8*, 1641. (c) Jiang, B.; Yang, S. W.; Bailey, S. L.; Hermans, L. G.; Niver, R. A.; Bolcar, M. A.; Jones, W. E., Jr. *Coord. Chem. Rev.* **1998**, *171*, 365. (d) Wang, B.; Wasielewski, M. R. *J. Am. Chem. Soc.* **1997**, *119*, 12. (e) Wolf, O.; Wrighton, M. S. *Chem. Mater.* **1994**, *6*, 1526. (f) Reddinger, J. L.; Reynolds, J. R. *Chem. Mater.* **1998**, *10*, 1236.

(3) (a) Kingsborough, R. P.; Swager, T. M. *Prog. Inorg. Chem.* **1999**, *48*, 123. (b) Zhu, S. S.; Swager, T. M. *J. Am. Chem. Soc.* **1997**, *119*, 12568. (c) Ley, K. D.; Whittle, C. E.; Bartberger, M. D.; Schanze, K. S. *J. Am. Chem. Soc.* **1997**, *119*, 3423. (d) Maruyama, T.; Yamamoto, T. *Synth. Met.* **1995**, *69*, 553. (e) Ley, K. D.; Schanze, K. S. *Coord. Chem. Rev.* **1998**, *171*, 287.

(4) (a) Kalyanasundaram, K. *Coord. Chem. Rev.* **1982**, *46*, 159. (b) Juris, A.; Balzani, F.; Barigelletti, F.; Campagna, S.; Belser, P.; Von Zelewsky, A. *Coord. Chem. Rev.* **1988**, *84*, 85. (c) Sauvage, J.-P.; Collin, J.-P.; Chambron, J.-C.; Guillerez, S.; Coudret, C.; Balzani, V.; Barigelletti, F.; De Cola, L.; Flamigni, L. *Chem. Rev.* **1994**, *94*, 993.

(5) (a) Meyer, T. J. *Acc. Chem. Res.* **1989**, *22*, 163. (b) Yamamoto, T.; Yoneda, Y.; Maruyama, T. *J. Chem. Soc. Chem. Commun.* **1992**, 1652. (c) Yu, S. Z.; Hou, S.; Chan, W. K. *Macromolecules* **2000**, *33*, 3259. (d) Lee, J.-K.; Yoo, D.; Rubner, M. F. *Chem. Mater.* **1997**, *9*, 1710. (e) Grigg, R.; Holmes, J. M.; Jones, S. K.; Norbert, W. D. *J. A. J. Chem. Soc., Chem. Commun.* **1994**, 185.

(6) (a) Yu, L.; Chan, W. K.; Peng, Z.; Gharavi, A. *Acc. Chem. Res.* **1996**, *29*, 13. (b) Wang, Q.; Wang, L.; Yu, L. *Macromol. Rapid Commun.* **2000**, *21*, 723. (c) Wang, Q.; Wang, L.; Ng, M.; Yu, L. *Polym. Prepr.* **2000**, *41*(1), 781.

(7) (a) Wang, Q.; Wang, L.; Yu, J.; Yu, L. *Adv. Mater.* **2000**, *12*, 974. (b) Wang, Q.; Wang, L.; Yu, L. *Polym. Prepr.* **1999**, *40*(2), 1309.

the redox and optical properties of the resulting materials depend significantly on the structures of the ligands. These polymers were shown to be photoconductive over a wide range of composition.

Experimental Section

Materials. Tetrahydrofuran (THF) was distilled from Na⁺/benzophenone ketyl. The *p*-divinylbenzene was separated from a mixture of *p*-divinylbenzene and *m*-divinylbenzene according to the literature procedure.⁸ All of the other chemicals were purchased from the Alderich Chemical Co. and used without further purification unless otherwise noted. The ligands used in this study are acetylacetonate (acac), 1,1,1-trifluoroacetylacetonate (tfac), 1,1,1,5,5,5-hexafluoroacetylacetonate (hfac), 4,4,4-trifluoro-1-phenyl-1,3-butanedione (tfpc), and 8-hydroxyquinoline (hyqu).

Synthesis of Monomers. Compound **1** and **3** were prepared by methods described previously.^{1c}

Compound 2a. A solution of 0.103 g of compound **1** (0.131 mmol) in 15 mL of methoxyethanol was heated to 80 °C. *cis*-Dichlorobis-(2,2'-bipyridine)ruthenium(II) hydrate (0.063 g, 0.131 mmol) in ethanol (10 mL) was added. The ethanol was then evaporated, and the resulting solution was stirred at 140 °C for 4 h. After cooling to room temperature, the solution was added into an (NH₄)PF₆ (0.213 g, 1.30 mmol) aqueous solution. The solid precipitated out and was purified by chromatography (silica gel, dichloromethane/methanol (20:1)) to yield 0.135 g (54%) of red-orange solid. ¹H NMR (CDCl₃, 400 MHz) δ 8.41 (m, 6H), 8.38 (d, 2H, *J* = 8.79 Hz), 7.95 (d, 4H, *J* = 8.37 Hz), 7.76 (dd, 4H, *J* = 5.10 Hz), 7.63 (s, 2H), 7.56 (s, 2H), 7.46 (m, 4H), 7.42 (s, 2H), 7.30 (d, 2H, *J* = 16.42 Hz), 6.79 (d, 2H, *J* = 16.42 Hz), 2.53–2.64 (m, 8H), 1.18–1.48 (m, 64H), 0.85 (t, 12H, *J* = 6.54 Hz). Elemental Anal. Calcd for C₈₆H₁₁₄N₂I₂P₂F₁₂Ru: C, 55.04; H, 6.07; N, 4.48; I, 13.52; Ru, 5.39. Found: C, 55.08; H, 6.12; N, 4.47; I, 13.60; Ru, 5.27.

General Procedure for Compounds 2b–f. To a solution of compound **1** in 10 mL of chloroform was added 2 equiv of hydrated ruthenium trichloride in 3 mL of ethanol. The resulting reddish brown solution was heated at 60 °C for 4 h and the color of the solution turned dark green. After removal of the solvent, the residue was separated by filtration chromatography (silica gel, dichloromethane/methanol (100:3)) to give a greenish solid. This greenish solid, triethylamine (1 equiv), and acetylacetonate (4 equiv) were then combined in 8 mL of THF and heated at 60 °C for 3 h, after which time the resulting mixture was poured into water. The mixture was extracted with dichloromethane. The combined organic layer was washed with water and dried over MgSO₄. The solvent was removed by rotary evaporation, and the residue was chromatographed on neutral alumina (Brockmann activity IV) with hexane/dichloromethane (2:1) as eluent to afford the desired compound.

Compound 2b: 42% of green-brown solid. ¹H NMR (CDCl₃, 400 MHz) δ 8.91 (s, 2H), 7.90 (d, 2H, *J* = 8.48 Hz), 7.63 (s, 2H), 7.56 (d, 2H, *J* = 7.81 Hz), 7.39 (s, 2H), 7.31 (d, 2H, *J* = 16.10 Hz), 6.94 (d, 2H, *J* = 16.09 Hz), 5.37 (s, 2H), 2.62–2.70 (m, 8H), 2.22 (s, 6H), 1.71 (s, 6H), 1.25–1.52 (m, 64H), 0.88 (m, 12H). Elemental Anal. Calcd for C₇₆H₁₁₂N₂I₂O₄Ru: C, 62.02; H, 7.61; N, 1.90; I, 17.25; Ru, 6.87. Found: C, 61.86; H, 7.57; N, 1.84; I, 17.14; Ru, 6.75.

Compound 2c: 51% of green solid. ¹H NMR (CDCl₃, 400 MHz) δ 8.72 (s, 2H), 7.80 (d, 2H, *J* = 8.42 Hz), 7.61 (m, 4H), 7.37 (s, 2H), 7.31 (d, 2H, *J* = 16.11 Hz), 6.93 (d, 2H, *J* = 16.09 Hz), 5.78 (s, 2H), 2.60–2.67 (m, 8H), 2.29 (s, 6H), 1.25–1.52 (m, 64H), 0.86 (m, 12H). Elemental Anal. Calcd for C₇₆H₁₀₆N₂I₂O₄F₆Ru: C, 57.78; H, 6.71; N, 1.77; I, 16.07; Ru, 6.40. Found: C, 57.90; H, 6.80; N, 1.78; I, 16.13; Ru, 6.30.

Compound 2d: 47% of brown solid. ¹H NMR (CDCl₃, 400 MHz) δ 8.67 (s, 2H), 8.06 (d, 2H, *J* = 8.46 Hz), 7.89 (d, 2H, *J* = 8.45 Hz), 7.66 (s, 2H), 7.45 (d, 2H, *J* = 16.49 Hz), 7.41 (s, 2H), 6.96 (d, 2H, *J* = 16.10 Hz), 6.17 (s, 2H), 2.63–2.71 (m, 8H), 1.26–1.54 (m, 64H), 0.86 (m, 12H). Elemental Anal. Calcd for C₇₆H₁₀₀N₂I₂O₄F₁₂Ru: C, 54.08; H, 5.92; N, 1.66; I, 15.04; Ru, 5.99. Found: C, 53.87; H, 5.78; N, 1.60; I, 14.92; Ru, 5.89.

Compound 2e: 40% of green-brown solid. ¹H NMR (CDCl₃, 400 MHz) δ 8.79 (s, 2H), 8.01 (m, 6H), 7.73 (d, 2H, *J* = 8.40 Hz), 7.57 (s, 2H), 7.50 (m, 2H), 7.41 (m, 4H), 7.32 (s, 2H), 7.29 (d, 2H, *J* = 16.16 Hz), 6.87 (d, 2H, *J* = 16.10 Hz), 6.46 (s, 2H), 2.63 (t, 4H, *J* = 7.80 Hz), 2.47 (t, 4H, *J* = 7.64 Hz), 1.25–1.52 (m, 64H), 0.87 (m, 12H). Elemental Anal. Calcd for C₈₆H₁₁₀N₂I₂O₄F₆Ru: C, 60.62; H, 6.46; N, 1.64; I, 14.90; Ru, 5.93. Found: C, 60.49; H, 6.37; N, 1.62; I, 14.81; Ru, 5.85.

Compound 2f: 53% of green solid. ¹H NMR (CDCl₃, 400 MHz) δ 10.40 (s, 2H), 8.13 (d, 2H, *J* = 8.48 Hz), 7.95 (d, 2H, *J* = 9.21 Hz), 7.75 (d, 2H, *J* = 9.19 Hz), 7.63 (s, 2H), 7.55 (s, 2H), 7.51 (m, 6H), 7.34 (d, 2H, *J* = 16.10 Hz), 7.19 (s, 2H), 7.01 (d, 2H, *J* = 16.09 Hz), 6.59 (d, 2H, *J* = 15.37 Hz), 2.59–2.68 (m, 8H), 1.24–1.41 (m, 64H), 0.86 (m, 12H). Elemental Anal. Calcd for C₈₄H₁₁₀N₄I₂O₂Ru: C, 64.60; H, 7.04; N, 3.59; I, 16.25; Ru, 6.47. Found: C, 64.43; H, 7.07; N, 3.68; I, 15.98; Ru, 6.52.

Polymerization. A typical polymerization procedure follows: Tri-*n*-butylamine (0.16 mL, 0.67 mmol) was added to a mixture of compound **2a** (0.03 g, 0.016 mmol), compound **3** (0.112 g, 0.144 mmol), *p*-divinylbenzene (0.0208 g, 0.160 mmol), palladium acetate (1.4 mg, 0.0062 mmol), and tri-*o*-tolylphosphine (9.7 mg, 0.032 mmol) in 4 mL of DMF. The reaction mixture was stirred at 90 °C for 5 h under a nitrogen atmosphere and then poured into methanol. The precipitate was collected, redissolved in chloroform, and filtered to remove the catalyst residue. The filtrate was concentrated and precipitated into methanol, followed again by filtration and reprecipitation. The resulting polymer was further purified by extraction in a Soxhlet extractor with methanol for 24 h and then dried under a vacuum overnight.

Characterization. The ¹H NMR spectra were collected on a Bruker 400 MHz FT NMR spectrometer. The FTIR spectra were recorded on a Nicolet 20 SXB FTIR spectrometer. A Shimadzu UV-2401Pc spectrometer and a Shimadzu RF-5301 PC spectrofluorophotometer were used to record the absorption and emission spectra. The cyclic voltammetry was measured on an EG&G Princeton Applied Research potentiostat interfaced to a personal computer. The experiment was carried out with a platinum disk working electrode, a platinum wire counter electrode, and an Ag/Ag⁺ reference electrode. The supporting electrolyte used was 0.1 M tetrabutylammonium perchlorate in dried dichloromethane. The half-wave potential was calculated using the equation $E_{1/2} = (E_{p,a} + E_{p,c})/2$, where $E_{p,a}$ and $E_{p,c}$ are the peak anodic and peak cathodic potentials, respectively. Thermal analyses were performed by using the DSC-10 system from TA Instruments with a heating rate of 10 °C/min under a nitrogen atmosphere. Elemental analyses were performed by Atlantic Microlab, Inc. and Galbraith Laboratories, Inc. Molecular weights were measured with a Water GPC system using polystyrene as the standard and THF as the eluent. The photoconductivity was studied by measuring the voltage drop across a 1 MΩ resistor resulting from a photocurrent running through the sample.⁹ A He–Ne laser (632.8 nm), diode laser (690 nm), and semiconductor laser (780 nm) were used as the light sources, respectively. The laser powers were controlled at about 6 W/cm².

Results and Discussion

Monomer Synthesis. Scheme 1 outlines the approach to the syntheses of these mixed-ligand ruthenium complexes. Compound **1** (L) was heated with hydrated ruthenium(III) trichloride in chloroform/ethanol to generate intermediate ruthenium complex RuLCl₃. After filtration chromatography, the residue was placed in a THF solution with an excess amount of ligand and triethylamine and refluxed for several hours. The triethylamine serves both as a reducing agent toward the RuLCl₃ and a deprotonating agent for the β-diketone and hydroxyquinoline.¹⁰ The desirable product was purified by column chroma-

(9) Li, L.; Lee, J. Y.; Yang, Y.; Kumar, J.; Tripathy, S. K. *Appl. Phys. B* **1991**, *53*, 279.

(10) (a) Jameson, D. L.; Goldsby, K. A. *J. Org. Chem.* **1990**, *55*, 4992. (b) Bessel, C. A.; See, R. F.; Jameson, D. L.; Churchill, M. R.; Takeuchi, K. J. *J. Chem. Soc., Dalton Trans.* **1993**, 1563.

(8) Strey, B. T. *J. Polym. Sci. Part A* **1965**, *3*, 265.

Scheme 1. Synthesis of Complexes 2a–f

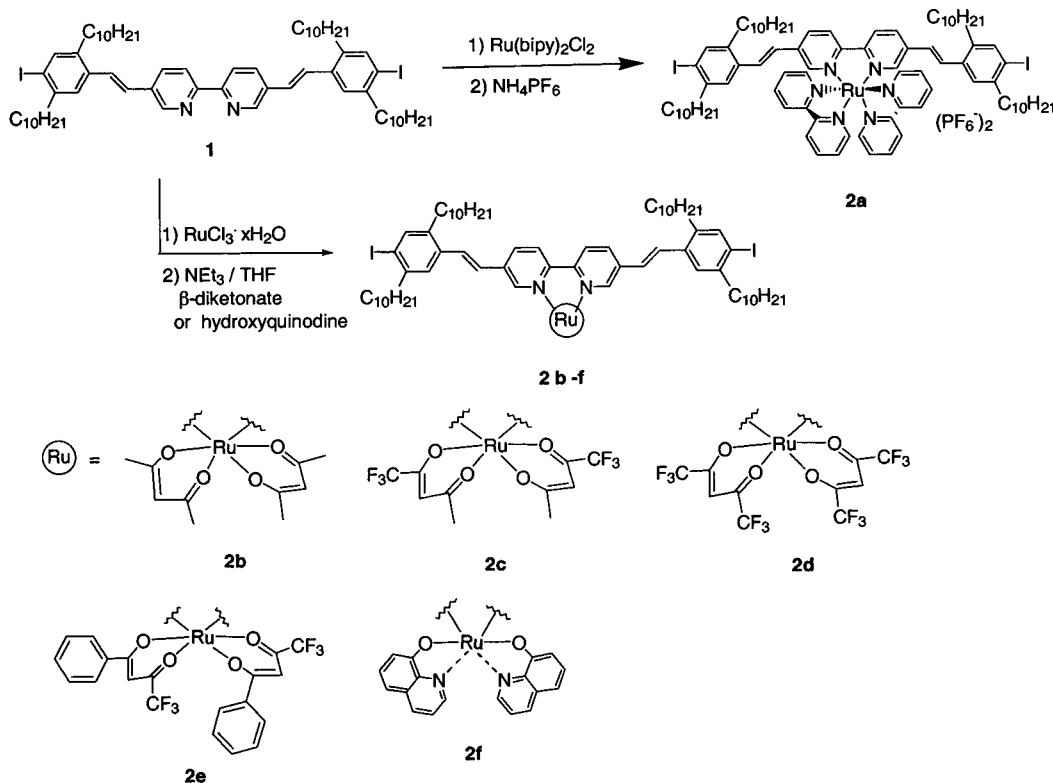


Table 1. Physical Properties of Complexes 2a–f

monomer	$\pi \rightarrow \pi^*$ (1) (nm)	$\pi \rightarrow \pi^*$ (2) (nm)	$E_{1/2}$ (V)	$\nu(\text{C}=\text{O})$ (cm^{-1})
2a	430		1.13	
2b	398	708		1526
2c	395	635	0.05	1590
2d	401	551	0.58	1592
2e	397	636	0.075	1570
2f	399	625	0.14	

tography on neutral alumina with hexane/dichloromethane as the eluent. Tris(bipyridyl) ruthenium complex (2a) was also synthesized for the purpose of comparison. The purity of these metal complexes was confirmed by elemental analysis.

Structural Characterization. The structures of these complexes were characterized both spectroscopically and analytically. The results from combustion analysis are consistent with all of the expected structures. It should be noted that the complexes with unsymmetrical ligands such as tfac and tfpc have geometrical isomers. However, discrimination between *trans*(CF₃)-*cis*(CH₃)-{RuL} and *cis*(CF₃)-*trans*(CH₃)-{RuL} as well as *trans*(CF₃)-*cis*(C₆H₅)-{RuL} and *cis*(CF₃)-*trans*(C₆H₅)-{RuL} is not possible from the NMR spectra, since both are of C₂ symmetry. Only one signal from the methine protons of tfac⁻ and tfpc⁻ ligands in their ¹H NMR spectra was observed for both complexes 2c and 2e.

The FTIR spectra of ruthenium acetylacetonato complexes (2b–e) showed very strong, characteristic absorption peaks corresponding to the C=O stretching mode, appearing around the 1526–1592 cm⁻¹ region depending on the substituents (Table 1).¹¹ For the complexes having trifluoromethyl substituents, the frequencies are higher for the absorption peaks than for the others. This trend is due to the stronger electron-

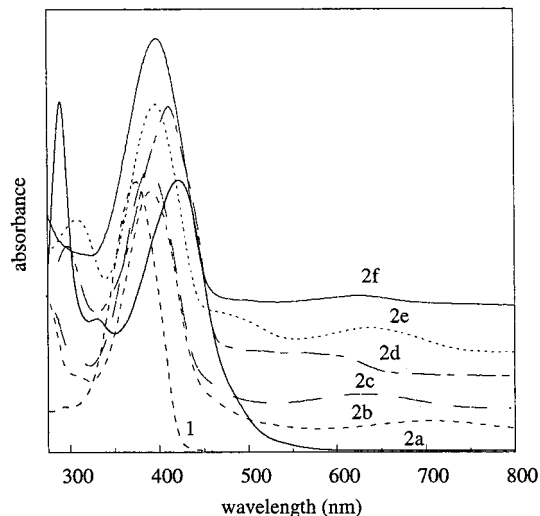


Figure 1. UV/vis spectra of compound 1 and complexes 2a–f in chloroform.

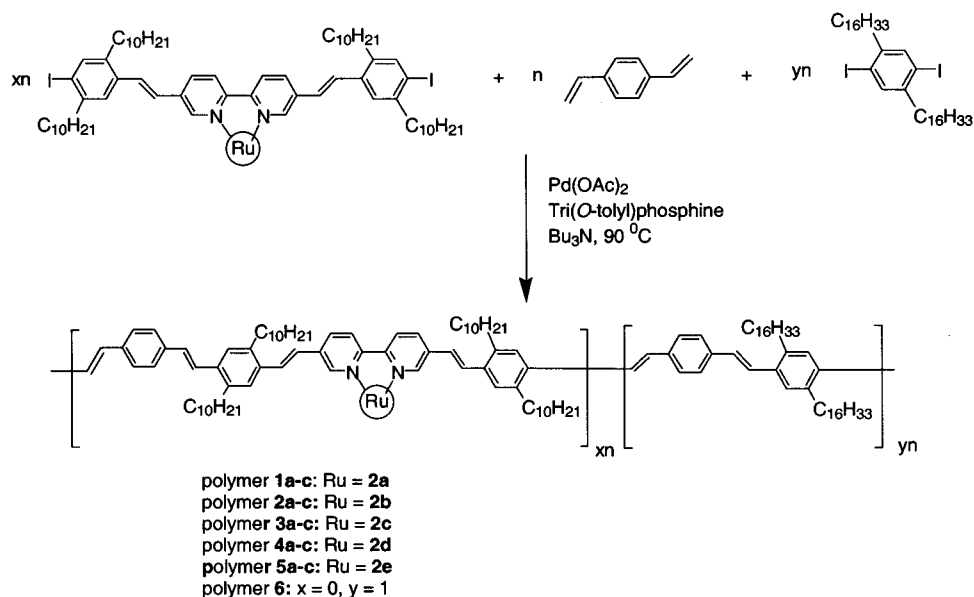
withdrawing power of the trifluoromethyl group relative to the CH₃ group, and the consequent strengthening of the C=O bonding.¹²

The UV/vis spectra of these complexes are presented in Figure 1. The $\pi\text{-}\pi^*$ transition at 374 nm, observed in compound 1, was red-shifted upon coordination to a metal ion ($\lambda_{\text{max}} = 395\text{--}423$ nm for complexes 2a–f). This shift is normally observed for π -conjugated systems and is ascribed to the effect of the positive charge on the energy levels of bpy. In complex 2a, a ligand-centered transition due to the bpy exists at around 285 nm. The absorption due to the metal-to-ligand charge transfer (MLCT) transition overlaps with that of the $\pi\text{-}\pi^*$

(11) Nakamoto, K. *Infrared and Raman Spectra of Inorganic and Coordination Compounds*, 4th ed.; Wiley: New York, 1986.

(12) (a) Mehrota, R. C.; Bohra, R.; Gaur, D. P. *Metal β -diketonates and Allied Derivatives*; Academic Press: San Francisco, 1978. (b) Holtzclow, H. F., Jr.; Collman, J. P. *J. Am. Chem. Soc.* **1957**, *79*, 3318.

Scheme 2. Polymerization Utilizing the Heck Coupling Reaction



transition. We can tentatively assign the $\pi-\pi^*$ transition at 423 nm and the MLCT transition at about 450 nm.^{1,4} In complexes **2b-f**, the intensities of bands arising from bpy-centered transition decreased dramatically. The MLCT bands further red-shifted toward lower energy ($\lambda_{\max} = 551-708$ nm) due to the reduction of the ligand-field strength. This is presumably due to a decreasing $M \rightarrow L$ π -interaction, which corresponds to an increase in the energy of the Ru($d\pi$) orbital. Acetylacetonate and phenolate groups are poor π -acceptors compared to the bpy ligand. The variation of ligands results in a range of MLCT energies. The complexes **2a-f** do not show luminescence at room temperature, although compound **1** exhibits strong emission peaks at 426 and 448 nm, a feature typical for dialkyl-substituted PPVs. The emission process is quenched after the Ru complexes are incorporated.

Polymer Synthesis and Characterization. From our previous studies and the work of other groups, the Heck coupling reaction was found to be effective in synthesizing functional conjugated polymers due to its mild condition.^{1,13} In this study, ruthenium complexes bearing diiodofunctional groups were copolymerized with 1,4-divinylbenzene and 1,4-diiodo-2,5-dihexadecanebenzene **3** in different stoichiometric ratio under the standard Heck reaction condition (Scheme 2). Dimethylformamide (DMF) was used as the solvent and the catalyst system was composed of palladium acetate (4 mol %), tributylamine (2.5 equiv), and tri-*o*-tolylphosphine (20 mol %). All of the ruthenium complexes except **2f** were able to survive in the polymerization condition. A series of PPV-type polymers with different ruthenium loading, ranging from 0 to 50%, were prepared and some of their physical properties are summarized in Table 2. It should be pointed out that the ruthenium complexes are randomly distributed along the polymer chains.

It was found that polymers **1a-c** are very soluble in polar aprotic solvent such as DMF, NMP, and DMSO due to the presence of ionic ruthenium complexes in the polymer chain. Polymers **2-5** containing neutral ruthenium complexes are readily soluble in chloroform, but they are sparingly soluble in

Table 2. Synthesis and Properties of Polymers 1-6

polymer	x	y	T_g (°C) ^a	T_d (°C) ^a	M_n	M_w	P_d
1a	0.1	0.9	65	294	16600	38000	2.29
1b	0.2	0.8	67	271	12800	20900	1.63
1c	0.5	0.5	64	245	9400	12500	1.33
2a	0.1	0.9	69	369	15200	28700	1.89
2b	0.2	0.8	66	310	11300	17600	1.56
2c	0.5	0.5	58	198	8900	12200	1.39
3a	0.1	0.9	49	365	15100	25400	1.68
3b	0.2	0.8	46	330	12200	17600	1.44
3c	0.5	0.5	47	207	10100	12200	1.21
4a	0.1	0.9	57	290	11800	17700	1.50
4b	0.2	0.8	59	245	9000	12400	1.38
4c	0.5	0.5	—	171	7400	8660	1.17
5a	0.1	0.9	43	208	13700	23700	1.73
5b	0.2	0.8	46	180	10800	16100	1.49
5c	0.5	0.5	—	167	8560	10400	1.22
6	0	1	56	380	18300	43900	2.40

^a T_g : glass transition temperature. —: not observed. T_d : decomposition temperature.

DMF. The molecular weights of these polymers were characterized using GPC, based on polystyrene as the standard (Table 2). The molecular weights of all of the polymers are not very high but are high enough to prepare uniform films.

The structures of the polymers were characterized by different spectroscopic techniques. The ¹H NMR spectra of these polymers generally feature the chemical shifts of the dialkyl-substituted PPV backbone. For example, the chemical shifts at 7.5 and 7.3 ppm correspond to the aromatic protons on the phenyl ring. The chemical shifts due to vinyl protons appear around 7.1 ppm. The remaining peaks in the range of 0.9–2.7 ppm correspond to the alkyl side chains. The protons from metal complexes can still be observed, depending on the polymers' composition (Figure 2). The chemical shifts at 9.0–8.0 ppm can be assigned to the bipyridyl protons in the conjugated backbone. Resonance from γ -H in diketone ligands can be found in the range of 5.4–6.6 ppm. The integration of the corresponding protons indicates the composition of the polymer, which is consistent with the ratios of the monomers.

Absorption spectra of these polymers feature a strong band at $\lambda_{\max} \approx 400$ nm which is assigned to the $\pi-\pi^*$ transition of the polymer backbone. The presence of the ruthenium metal complexes is manifest by the appearance of a lowest energy

(13) (a) Heitz, W.; Brugging, W.; Freund, L.; Gailberger, M.; Greiner, A.; Jung, H.; Kampschulte, U.; Niebner, N.; Osan, F. *Makromol. Chem.* **1991**, *192*, 967. (b) Suzuki, M.; Lim, J. C.; Saegusa, T. *Macromolecules* **1990**, *23*, 1574. (c) Weitzel, H. P.; Mullen, K. *Makromol. Chem.* **1990**, *191*, 2837. (d) Bao, Z.; Chen, Y.; Cai, R.; Yu, L. *Macromolecules* **1993**, *26*, 5281. (e) Bao, Z.; Chen, Y.; Yu, L. *Macromolecules* **1994**, *27*, 4629.

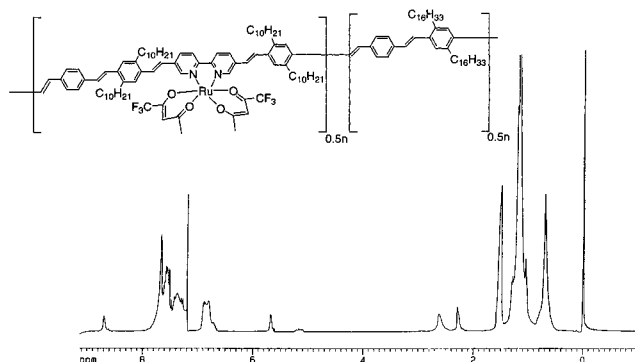


Figure 2. The ^1H NMR spectrum of polymer **3c**.

MLCT band associated with different metal complexes. The delocalized nature of the π^* acceptor orbital in the polymers is evident from an ca. 12–50 nm red shift of the MLCT transition relative to the position in the corresponding monomer. The intensity of the MLCT band increases (relative to the π – π^* transition) with the increase of the ratio of the complex. This is a useful feature to control the polymer's optical properties. The absorption strength of the polymers at longer wavelengths can be adjusted by controlling the ratio of the monomers.

FTIR spectra of the polymers **2–5** show C=O bands at 1520–1600 cm^{-1} , further confirming that the diketonate ruthenium complexes were incorporated into polymers. The polymers **1a–c** exhibit typical absorption bands of pyridine moieties at 1620 cm^{-1} (triple absorption bands) and at 760 cm^{-1} . The intensities of these peaks are well correlated to the ruthenium complex composition. The intense band at 965 cm^{-1} for polymers **1–6** is ascribed to the out-of-plane bending vibration of the trans-substituted vinylene group.

The thermal properties of these polymers were examined by differential scanning calorimetry (DSC) (Table 2). All of these polymers show a rather low glass transition temperature presumably due to the existence of long greasy side chains and the bulky metal complexes. It was found that the decomposition temperature of the polymers decreases as the ratio of metal complexes increases. The presence of the bulky ruthenium complexes may distort the packing of polymer chains and reduce the thermal stability of the polymer.

Cyclic Voltammetry. The redox properties of the complex monomers and polymers were studied by cyclic voltammetry (CV) in CH_2Cl_2 solution. Examination of the electrochemistry data reveals a number of interesting features. For complex **2a**, the reversible wave of the Ru(III/II) couple occurs at $E_{1/2} = 1.13$ V vs Ag^+/Ag in 0.1 M Bu_4NClO_4 /dichloromethane (Table 1). Under the same conditions, the reversible waves of the Ru(III/II) couple for complexes **2b–f** require much smaller voltage ($E_{1/2}$ between 0.012 and 0.58 V). Replacement of π -acidic pyridyl ligands by σ -donating diketonate and phenolate ligands results in a decrease in redox potential of the Ru(III/II) couple (and hence stabilization of the high oxidation state) by 1.118–0.55 V. The anionic β -diketonate and phenolate groups also neutralized the charge of the ruthenium ions, which results in additional electrostatic stabilization of the oxidation state. This is in agreement with the shift of the MLCT (metal oxidation) bands to lower energy by electron donation from the acetylacetonate and phenolate groups in UV/vis studies. The electrochemical data presented in Table 1 suggest that the electron density of the ruthenium center is strongly influenced by the electron-donating/withdrawing nature of the substitutes on β -diketonate ligands. The Ru(III/II) redox potentials shift in the anodic direction with the β -substituent on the diketonate

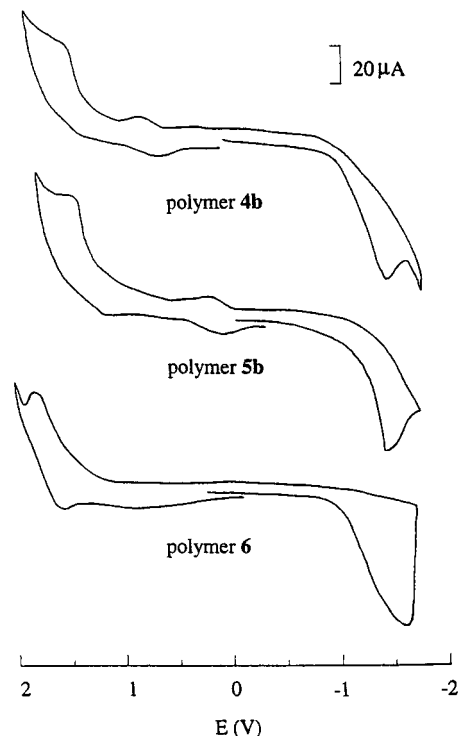


Figure 3. Cyclic voltammograms of polymers **4b**, **5b**, and **6**.

ligand in the following order: $\text{Me} < \text{Ph} < \text{CF}_3$. It was suggested that such a shift is largely due to inductive effect.¹⁴ Hence, variation of the substituents on ligands fine-tuned the redox potentials of these complexes.

The CV curves of the polymers **1–5** clearly showed the reversible metal-centered oxidation processes (Figure 3). It was found that the polymerization did not significantly alter the redox properties of the complex moieties compared to their corresponding monomers. However, the redox peaks corresponding to the conjugated backbone shift after the incorporation of the transition metal complexes. The irreversible cathodic peaks shifted from -1.78 V in polymer **6** to about -1.54 V in polymers **1–5**. The irreversible anodic peak appears around 1.42 V in polymers **1–5** while it appears at 1.58 V in polymer **6**. The irreversibility of these redox processes was also observed in other metal-containing conjugated polymers and may be due to the charge trapping in the polymer during the doping process.¹⁵

Photoconductivity. Photoconductivity is one of the informative phenomena for many organic semiconductors.¹⁶ Information about photogeneration, recombination, and transport processes of the charge carriers can be obtained. The MLCT process in the ruthenium complexes enables us to photoexcite the polymers at longer wavelengths. Upon excitation in the region of the MLCT transition of the ruthenium complex, electrons will be injected into the polymer backbone (equivalent of n-doping of PPV) and transported away through either intrachain migration or interchain hopping. It is well-known that oxidation or reduction (doping) of conjugated polymer backbones results in a highly conducting state of polymers (due to formation of so-

(14) (a) Holm, R. H.; O'Conner, M. J. *Prog. Inorg. Chem.* **1971**, *14*, 241. (b) Patterson, G. S.; Holm, R. H. *Inorg. Chem.* **1972**, *11*, 2285. (c) Takeuchi, T.; Endo, A.; Shimizu, K.; Sato, G. P. *J. Electroanal. Chem.* **1985**, *185*, 185.

(15) Chan, W. K.; Ng, P. K.; Gong, X.; Hou, S. *J. Mater. Chem.* **1999**, *2103*.

(16) Mylinikov, V. S. *Photoconducting Polymers in Advances in Polymers Science*; Springer-Verlag: Berlin, Heidelberg, 1994; Vol. 115.

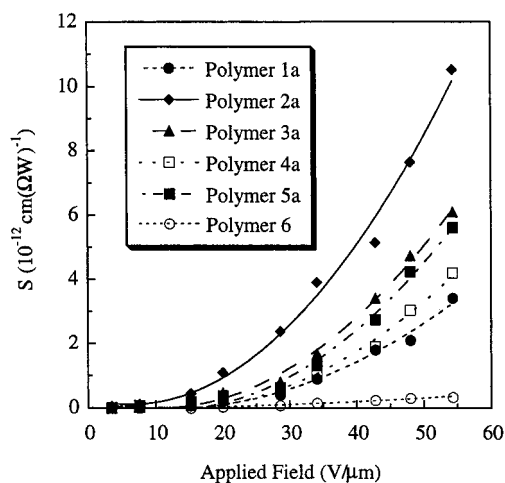


Figure 4. Photoconductive sensitivity of polymers **1a–6** as a function of the applied field. Polymers **1a** and **6** were excited at 632.8 nm. Polymer **4a** was excited at 690 nm. Polymers **2a**, **3a**, and **5a** were excited at 780 nm.

called polaron and bipolaron species).¹⁷ Thus, the charge-separation efficiency and photoconductivity can be greatly improved due to the combination of efficient photocharge generation and charge transport. The samples for photoconductivity measurement were prepared by casting a polymer solution onto an indium–tin oxide (ITO) glass. A thin layer of gold electrode (150 Å) was coated onto the polymer film by vacuum deposition. The typical thickness of the polymer film was approximately 1 μm. The photocurrent was measured by monitoring the voltage drop on a resistor that is in series with the film capacitor. On the basis of their different MLCT bands, the polymers were excited by different wavelengths of the light sources, where they have similar absorption coefficients. For example, polymers **1a** and **6** were excited by a He–Ne laser (632.8 nm). Polymer **4a** was excited with a diode laser (690 nm), while polymers **2a**, **3a**, and **5a** were illuminated with a semiconductor laser (780 nm). As shown in Figure 4, the photoconductive sensitivity (*S*) strongly depends on the applied field and exhibits trends well correlated with the CV results of the complexes.¹⁸ The lower the oxidation potential of the polymer will be, the higher the photoconductive sensitivity of the polymer will be. Compared to polymer **1**, polymers containing ruthenium acetylacetonato complexes exhibit much higher photosensitivity. The photoconductivity of the polymers also appears to be dependent on the ruthenium content in the polymer. Under the same electric field strength, the conductivity increases as the ruthenium content is increased (Figure 5). The photoconductive response of polymers to different wavelength resembles their MLCT absorption spectra (Figure 6). The above results clearly confirm that the ruthenium complexes extend the photosensitivity of the polymers to the region of longer wavelengths through the presence of their lowest energy MLCT band.

(17) Bredas, J. L., Silbey, R., Eds. *Conjugated Polymers*; Kluwer Academic Publishers: Dordrecht, The Netherlands, 1991.

(18) Schildkraut, J. S. *Appl. Phys. Lett.* **1991**, *58*, 340.

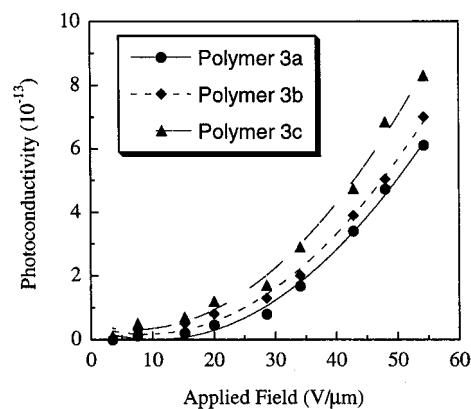


Figure 5. Dependence of photoconductivity on the applied field for polymers **3a–c** at 780 nm.

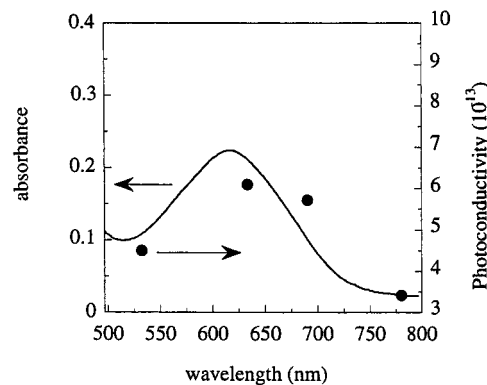


Figure 6. Photoconductivity and absorption spectrum of polymer **3a** in the visible region.

Conclusions

A series of novel ruthenium complexes containing β -diketonate ligands have been synthesized and incorporated into conjugated polymer backbone. Their redox and optical properties have been measured and were shown to be significantly dependent on the structures of the ligands. The bidentate β -diketonate ligand substantially lowers the Ru(III/II) potentials relative to analogous polypyridyl complexes. A wide range of lowest energy MLCT bands has been observed in these ruthenium complexes. Upon excitation in the MLCT range, these polymers exhibited interesting photoconductivity. The design approach presented here demonstrates the feasibility of varying the structures of the ligands to fine-tune the physical properties of the resulting materials and can be used for preparing other kinds of transition metal complexes. This approach also opens the way for a regulation of photosensitivity of conjugated polymers over a wide range to match the laser wavelength for the desired application.

Acknowledgment. We gratefully acknowledge the financial support of the National Science Foundation and the Air Force Office of Scientific Research. This work also benefited from the support of the NSF MERSEC program at the University of Chicago.

JA003140H